Quaternary Science Reviews 77 (2013) 31–45

Contents lists available at SciVerse ScienceDirect

Quaternary Science Reviews

journal homepage: www.elsevier.com/locate/quascirev

A two-step expansion of the dinocyst *Lingulodinium machaerophorum* in the Caspian Sea: the role of changing environment☆

S.A.G. Leroy [a,*], H.A.K. Lahijani [b], J.-L. Reyss [c], F. Chalié [d], S. Haghani [a,b,e], M. Shah-Hosseini [b,d], S. Shahkarami [b,e], A. Tudryn [f], K. Arpe [a,g], P. Habibi [b], H.S. Nasrollahzadeh [h], A. Makhlough [h]

[a] *Institute for the Environment, Brunel University, Kingston Lane, Uxbridge UB8 3PH, West London, UK*
[b] *Iranian National Institute for Oceanography (INIO), No 3, Etemadzadeh St., Fatemi Av., Tehran 1411813389, Iran*
[c] *Laboratoire des Sciences du Climat et de l'Environnement, CEA-CNRS, Avenue de la Terrasse, F-91198 Gif-sur-Yvette Cedex, France*
[d] *Aix-Marseille Université, CEREGE, UMR-7330 CNRS, UM34, 13545 Aix-en-Provence Cedex 04, France*
[e] *School of Geology, University of Tehran, Enghelab Sq., Tehran, Iran*
[f] *Laboratoire CNRS/UPS UMR 8148 IDES, Université de Paris XI, Département des Sciences de la Terre, Bâtiment 504, 91 405 ORSAY Cedex, France*
[g] *Max Plank Institute for Meteorology, Hamburg, Germany*
[h] *Ecology Departments, Caspian Sea Ecology Research Center (CSERC), 961 Sari, Iran*

ARTICLE INFO

Article history:
Received 13 March 2013
Received in revised form
18 June 2013
Accepted 27 June 2013
Available online 4 August 2013

Keywords:
Caspian Sea
Dinocysts
Past sea surface temperature
Last centuries
Last millennia

ABSTRACT

Dinoflagellate cyst assemblages were analysed in four short sediment cores collected in the south Basin of the Caspian Sea for assessing environmental changes over the last few millennia. Two of these cores were dated by radionuclides. The sedimentation rate of one of them was very high, in the order of 20 mm per year. The interpretation of the four sequences is supported by a collection of 27 lagoonal or marine surface sediment samples. A sharp increase in the concentration of the dinocyst occurs after 1967, especially owing to *Lingulodinium machaerophorum*. Considering nine other cores covering parts or the whole of Holocene, it became clear that this species started to develop in the Caspian Sea only during the last three millennia. By analysing instrumental data and collating existing reconstructions of sea level changes over the last decades, we show that the main forcing for the recent increase of *L. machaerophorum* percentages and concentration is global climate change, especially sea surface temperature increase. Sea level fluctuations likely only have a minor impact. We argue that the recent increase in *L. machaerophorum* indicates that the Caspian Sea clearly is in the Anthropocene.

1. Introduction

The Caspian Sea (CS), with a surface area larger than that of the British Isles, is the largest inland water body in the world (Fig. 1). This lake is well known for the petroleum and caviar it produces. Its ecosystem, which is unique owing to many endemic species, is under increasing pressure. The monitoring of its ecosystem changes is inconsistent across the five riparian countries, because of their different socio-economical levels; so an accurate overview of the environmental changes affecting ecosystem processes at present is not available. The instrumental records of the last century indicate rapid changes in sea surface temperature, in sea level and in trophic levels. Sea level changes are large, close to 3 m amplitude and a hundred times faster than that of the global ocean in the 20th century (Crétaux and Birkett, 2006; Fig. 2A), but also as much as 20 m amplitude in the last few millennia (Kakroodi et al., 2012). The sea surface temperature of the south basin especially in the summer shows a warming trend over the last century (Ginzburg et al., 2005).

The use of dinocyst-inferred reconstruction of past water parameters, such as temperature, salinity, and nutrient levels, is a commonly used as a powerful semi-quantitative palaeoenvironmental approach (Marret and Zonneveld, 2003); however this technique is still in its infancy in the Caspian Sea (Leroy et al., 2006, 2011).

Using four short sediment cores (36–166 cm long) and 27 surface samples taken in the south basin and adjacent areas, the aims of this paper are 1) to establish a preliminary spatial distribution

* Corresponding author. Tel.: +44 1895 266 087; fax: +44 1895 269 761.
E-mail address: suzanne.leroy@brunel.ac.uk (S.A.G. Leroy).

0277-3791/$ – see front matter © 2013 The Authors. Published by Elsevier Ltd. All rights reserved.
http://dx.doi.org/10.1016/j.quascirev.2013.06.026

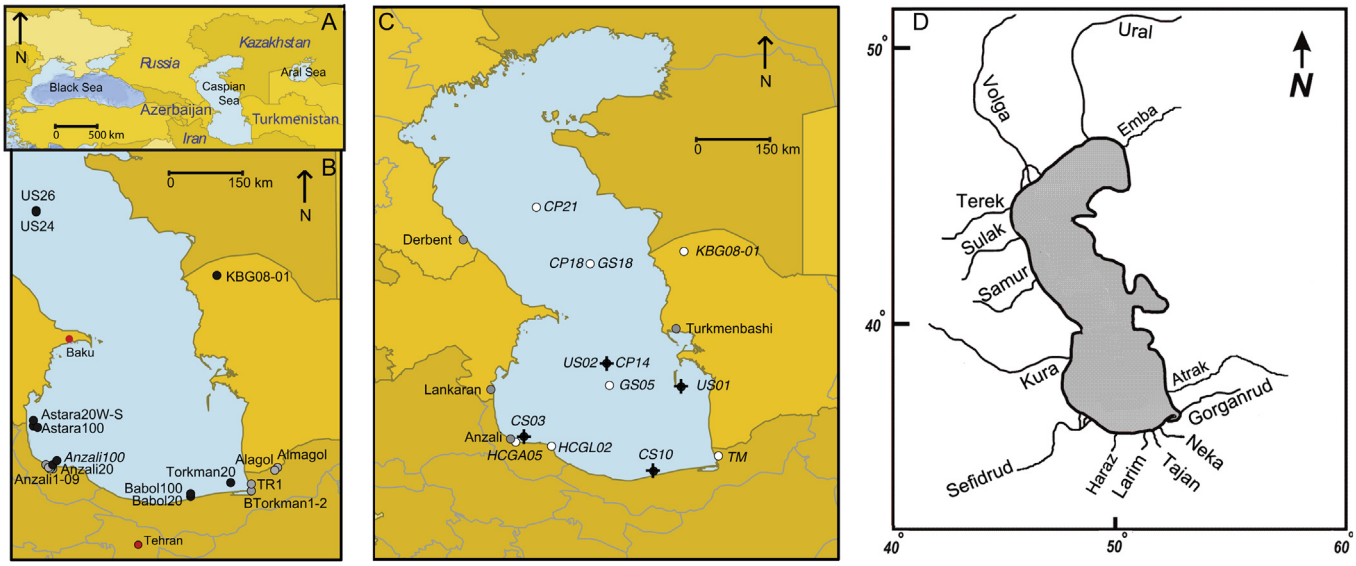

Fig. 1. Location maps. (A): Location of the Caspian Sea at the boarder between Europe and Asia. (B): Location of the surface samples in the Caspian Sea (black dots for marine samples and grey dots for lagoonal samples), and capital cities (red dots). (C): Location of the four short cores (black dots with cross), the other Caspian cores (white dots) and the meteorological stations (grey dots). (D): Main rivers flowing to the Caspian Sea. (For interpretation of the references to colour in this figure legend, the reader is referred to the web version of this article.)

pattern of dinoflagellate cysts in the Caspian area, especially the south basin; 2) to detect and explain changes over the last century in dinocyst assemblages and 3) set it in the context of the Holocene – Neocaspian period. Prime focus will be on the stepwise changes in percentages and concentration of the autotrophic dinocyst *Lingulodinium machaerophorum* (Deflandre and Cookson, 1955) Wall, 1967, subsequently called *Lmac* (abbreviation as in Zonneveld et al., 2013), which is a euryhaline coastal planktonic species restricted to regions with summer temperatures above 10–12 °C and winter temperatures above 0 °C (Lewis and Hallett, 1997). Its motile form, *Lingulodinium polyedrum* (Stein 1883) Dodge 1989, is reported to cause harmful algal blooms (Howard et al., 2009). This species therefore is sensitive to sea surface temperature and could be used to reflect climatic change in the region.

The impact of this work is important in advancing knowledge of CS processes. The CS holds a dominant position in the southwestern Asian region, and is suspected of playing a major part in climate change in this part of the world. However, a lack of a clear understanding of the processes involved in its control such as the North Atlantic Oscillation or the El-Niño Southern Oscillation still exists not only for the last few millennia but also for the last few decades (Arpe et al., 2000, 2012; Arpe and Leroy, 2007). This paper addresses the issue of past temperatures and develops basic data that will underpin future work on CS climate-related aspects.

2. Setting

For two out of the four coring locations more local information is provided in Appendix A.

2.1. Geographical setting and climate

The CS is the world's largest inland water body in terms of both area and volume, extending 35–48°N and 47–55°E. The altitude of the surface lays around 26 m bsl (25–29 m bsl during the last 150 yr) (Leroy et al., 2006; Arpe et al., 2012). The sea is divided into three basins, becoming deeper southwards: the northern basin (80,000 km^2) with an average depth of 5 m and a maximum depth of 15 m; the middle basin (138,000 km^2) with an average depth of 175 m and a maximum depth of 788 m; and the southern basin (168,000 km^2) with an average depth of 325 m and a maximum depth of 1025 m. The southern basin holds more than 65% of the Caspian water. In 1951, the CS was artificially reconnected to the Black Sea via the Volga-Don canal open.

Because of its great meridional extension (>1100 km), the CS straddles several climatic zones (Kosarev, 2005). The northern part of the drainage basin lies in a zone of temperate continental climate with the Volga catchment well into the humid mid-latitudes. The western coast features a moderately warm climate, while the southwestern and the southern regions fall into a subtropical humid climatic zone. The eastern coast has a desert climate.

2.2. Currents, salinity and temperature

A complex sea current pattern in the middle and south basins is dominated by a surface cyclonic gyre (Zenkevitch, 1963). Specifically in the South Caspian, a dipole system, consisting of an anticyclonic gyre in its northwestern part and a cyclonic gyre in its southeastern part, exists throughout the year (Zaker et al., 2011). The sea currents influence the four studied sites as they have potential to transport fine-grained materials. In contrast to the east coast of the middle basin, no upwelling develops in the south basin (Tuzhilkin and Kozarev, 2005).

In general, at the scale of the CS, the summer gradient of salinity is stronger than that of the winter. The main influences are, on an otherwise relatively stable salinity around 11–12 psu, the freshening influence of the Volga River in the north basin (salinities less than 1 psu), and the stronger evaporation in the southeast (salinities up to 14 psu) (Kosarev and Yablonskaya, 1994; Dumont, 1998). Monitoring from 1956 to 2000 shows high salinities in the early 1970s and low salinities in the early 1990s, corresponding respectively to low annual river discharge and high annual river discharge as well as the 1977 lowstand and the 1995 highstand (Fig. 2A). This water level change caused respectively a mixing of the water column and a stratification of the water column (Tuzhilkin and Kozarev, 2005). In the south basin, the summer and winter gradients show that the west is fresher (12.2 psu) and the east more saline (13.8 psu).

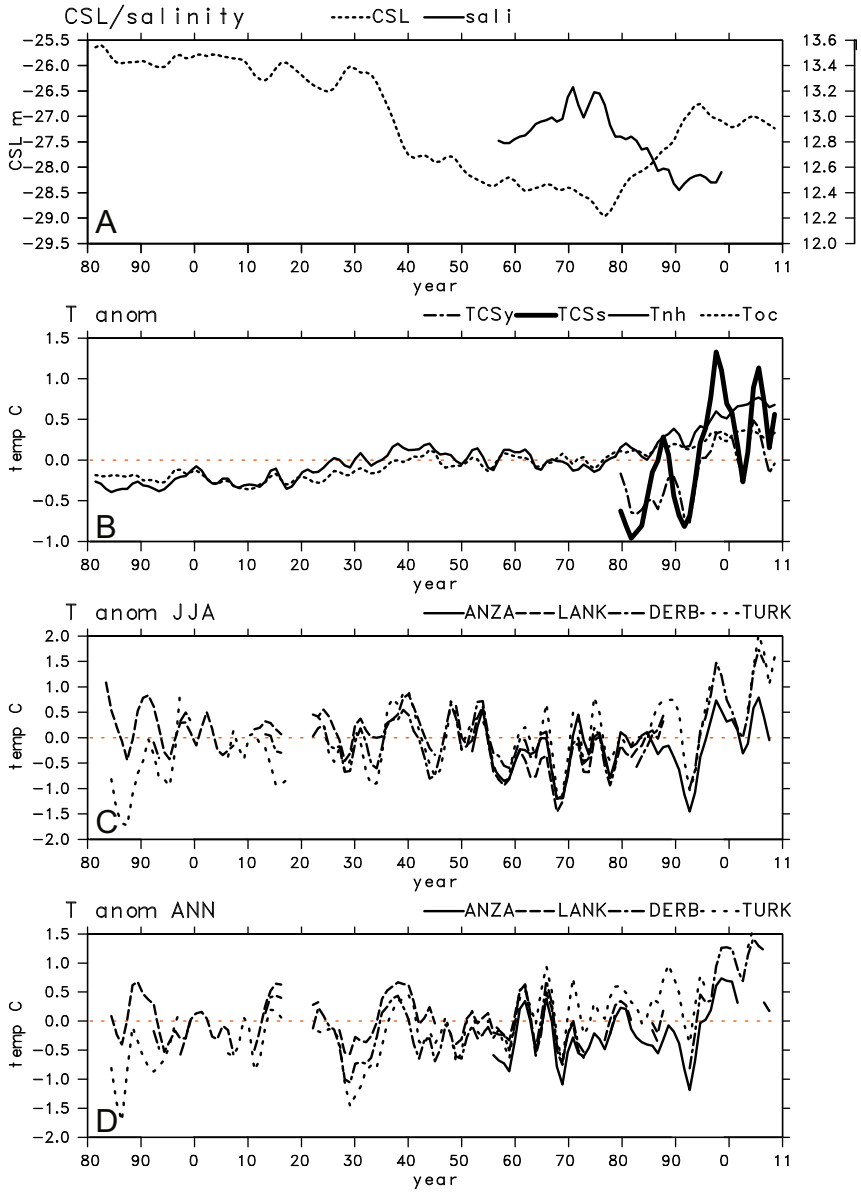

Fig. 2. Selected oceanographic and meteorological data for the Caspian Sea. All data are smoothed with a 1-2-1 filter. Anomalies are used for panels 2B, 2C and 2D. (A): Caspian Sea level (CSL) (Golitsyn and Panin, 1989; Cazenave et al., 1997; USDA, no date) and summer surface salinity from the centre of the middle basin (sali) (Tuzhilkin and Kozarev, 2005). (B): Sea surface temperatures of southern Caspian Sea from analysis (TCSy = CS year-Jan.–Dec.; TCSs = CS summer-JJA.) (Dee et al., 2011); Annual mean 2 m temperatures of the northern hemisphere (Tnh) and annual mean of global ocean temperatures (Toc) (NASA, no date). (C): 2 m temperatures in summer (JJA) for the following meteorological stations (Climatic Research Unit, University of East Anglia, no date): ANZA = 407180, 37.5N 49.5E, −26 m asl, Anzali, Iran LANK = 379850, 38.7N 48.8E, −12 m asl, Lankaran, Azerbaijan DERB = 374700, 42.0N 48.3E, −19 m asl, Derbent, Russia TURK = 385070, 40.1N 53.0E, 82 m asl, Turkmenbashi, Turkmenistan. (D): Annual 2 m temperatures for stations in 2C (Climatic Research Unit, University of East Anglia, no date).

In the CS, summer temperature varies from 26 °C in the NW to >28 °C in the SE. Winter temperatures are 10 °C in the centre of the basin and get cooler by 2–3 °C towards the periphery. A record of sea surface temperature in the south CS from 1982 to 2011 obtained by satellite (Fig. 2B) shows a clear warming trend for all seasons (0.10 °C yr^{-1}) by 1–2 °C and stronger for the south basin of the Caspian than the other regions (Ginzburg et al., 2005 updated by European Centre for Medium-Range Weather Forecasts, ECMWF). The warming is the strongest for the summer with an increase from a little less than 25 °C to more than 28 °C. The extreme summer maxima show the strongest increase (Ginzburg et al., 2005). A similar analysis for the whole CS shows the same positive trend in the yearly averaged SST (Kavak, 2012).

Moreover, based on hydrological data, a positive trend in the period 1900–1982 has been found but not as fast as after 1982 (Ginzburg et al., 2005). Thus the warming trend is independent of the significant sea level fluctuations that have taken place during the 20th century. A similar effect was observed in the Black Sea, Aral Sea and the Karabogaz-Gol by Ginzburg et al. (2005). These authors suggest that this warming trend could be a consequence of global warming (Fig. 2C). The sea ice season and extent in the northern basin have decreased for the period 1978–2002, also possibly related to global warming (Kouraev et al., 2004).

2.3. Nutrients and phytoplankton

Most **nutrients** enter the CS via the Volga River, hence the northern basin has the highest primary productivity. In the CS, the relatively low nutrient levels (Dumont, 1998) in the upper 100 m

are depleted by phytoplankton activity, but the nutrient concentrations increase with depth (Kosarev and Yablonskaya, 1994). Iranian lagoons and coastal regions have moreover been steadily polluted by anthropogenic sources (fertilizers and pesticides used in agriculture and increased nutrient load of river flows due to deforestation of woodland) since the early 1980s (Kideys et al., 2008).

Changes in phytoplankton biomass are one way to assess changes in water quality. Kideys et al. (2008) detected by satellite imagery an increase in chlorophyll a in the southern CS since 2001. The invasion of the comb jelly *Mnemiopsis leidyi* in the late 1990s caused a drop in zooplankton, which in turn favoured phytoplankton. But other factors such as overfishing, eutrophication and climatic change may also have played a role (Kideys et al., 2008). A similar analysis for the whole of the CS (Kavak, 2012) shows clearly a positive trend in chlorophyll a from 1998 to 2009.

The status of the south coast of the CS has changed between 1994 and 2005 from oligotrophic to meso-eutrophic (Nasrollahzadeh et al., 2008a,b; Bagheri et al., 2012). In 2006, an anomalous algal **bloom**, mostly due to a dinoflagellate *Heterocapsa*, occurred in front of Anzali harbour (Bagheri et al., 2011). Other algal blooms mostly due to the toxic Cyanobacteria *Nodularia spumigena* occurred in August and September 2005 (20,000 km^2 of the southern basin) (Soloviev, 2005), in August 2009 (off Tonekabon) and in July and early August 2010 (from Nowshahr to near Babolsar and offshore Anzali) (Makhlough et al., 2011; Nasrollahzadeh et al., 2011). It is noteworthy that *L. polyedrum* contributed significantly to the 2009 bloom (Nasrollahzadeh et al., 2011).

Despite these environmental changes, the CS is moderately meso-eutrophic, and mainly since 2001. This increase is mostly limited to its coastline, closest to densely populated areas.

2.4. Sediment sources and sedimentation rates

At present, rivers flowing to the northern Caspian coast (the Volga, Ural, Terek and Sulak) supply approximately 90% of the riverine water influx to the CS, whereas the southwestern and southern rivers (the Sefidrud, Kura and Gorganrud) are the main sources of sediments for the whole of the CS (Lahijani et al., 2008).

Studies of the CS sediment composition have so far focused on the northern basin, where the proportions of the different inputs were estimated to be 35% fluvial, 28% aeolian, 29% biogenic carbonate and 8% chemical carbonates (Khrustalyov and Artiukhin, 1992). The Iranian mountains, such as the Elburz Mountain, represent the main source of terrigenous materials in the south basin. The sediment has two main primary detrital sources, more siliciclastic in the west, more carbonates in the east (Lahijani and Tavakoli, 2012). One other source is aeolian transport by numerous dust storms from Turkmenistan, where Mesozoic limestones exist in the Kopet Dag (Lahijani and Tavakoli, 2012).

The south part of the basin was subsiding at a rate of the order of >1 mm yr^{-1} (Einsele and Hinderer, 1997) and this is probably still the case today.

The sedimentation rates in the south basin have always been very high due to its large accommodation space, strong erosion of the surroundings and orogenesis as well as aeolian inputs. For the Cainozoic, the sedimentary deposits in the southern Caspian basin are as much as 20–30 km thick, making it one of the deepest basins in the world. For the Pliocene–Quaternary time alone, 10 km of sediment have been deposited, providing an average accumulation rate close to 2 mm per year (Nadirov et al., 1997; Tagiyev et al., 1997). The sedimentation rate of the Pliocene in the south basin (the Pliocene Productive Series) is even higher up to 4 mm yr^{-1} (Kroonenberg et al., 2005).

2.5. Past dinocyst investigations in the Caspian Sea

Some modern samples from the Caspian region were published in Marret et al. (2004), which is also the reference paper for the description of a new Caspian genus, species and forms. Five surface samples were studied for their dinocyst content in the lagoon of Anzali (Kazancı et al., 2004) (Fig. 1).

The recent dinocyst history of the area is poorly known from previous dinocyst investigations, although four records cover the last 300 years at least (locations in Fig. 1): in the Amirkola and Anzali Lagoons (Leroy et al., 2011), in the Gomishan lagoon, S–E corner of the CS (Leroy et al., 2013) and in the Karabogaz Gol (Leroy et al., 2006).

3. Materials and methods

3.1. Collection of surface samples, coring and dating

Modern samples were derived from a combination of core tops, grabs and hand scooping (Appendix B). Sixteen samples came from marine settings, two from lakes, and nine from lagoons (locations in Fig. 1). Two Usnel boxes (50 cm thick) were taken in the south basin, during a French-Russian oceanographic cruise (August 1994), on board a Russian military ship, rented for the sea cruise (Appendix C). Box locations were in water depths of 13 m for core US01 and of 315 m for core US02. Cores from Usnel boxes were subsampled in PVC tubes on board and therefore contain the water–sediment interface. Two heavy Kajak gravity cores with a diameter of 5 cm, cores CS03 and CS10, were taken in 2007 from a boat rented by the Iranian National Institute for Oceanography (INIO) (Appendix C).

Two of the four cores were dated by radionuclides, i.e. US02 and CS03. ^{210}Pb, ^{226}Ra and ^{137}Cs records were obtained. Samples of core US02 were analysed every cm for both ^{210}Pb and ^{137}Cs in the top 10 cm, then every 2 cm down to 16 cm (results in Leroy et al., 2007). A sample at 22 cm reaches background values. For core CS03, samples were taken at c. 3 cm interval down to 60 cm and then at every c. 8 cm interval. Dry samples were measured with a very low-background, high-efficiency well-type detector located in the underground laboratory of Modane in the French Alps (Reyss et al., 1995) where 1700 m of rock overburden reduces the cosmic radiation by 6 orders of magnitude.

3.2. Sedimentology

For the sedimentary analysis of the two Usnels cores, dried samples were homogenized and representative subsamples were taken for grain size analysis by a LS 13 320 Multi-Wavelength Particle Size Analyzer, ASTM standard calibrated. Organic matter and calcium carbonate contents were determined by loss-on-ignition, bulk samples were dried at 105 °C for 24 h, then heated to 550 °C for 4 h to burn the organic matter, and organic free sample heated again to 950 °C for 8 h to break the calcium carbonate. The percentages of organic matter and calcium carbonate were then calculated by the method used by Dean (1974).

For the two Kajak cores, samples were homogenized and representative subsamples were taken for grain size analysis. The distribution for the fraction coarser than 1 mm was determined using the standard wet sieving procedure. Grain-size analysis for particles less than 1 mm was undertaken using a “Fritsch Analysette Comfort 22” Laser Particle Sizer. Organic matter was determined by wet digestion through oxidation in hydrogen peroxide on bulk

samples (Schumacher, 2002). The calcium carbonate was determined by using a Bernard calcimetre.

The magnetic susceptibility was measured with a Bartington Instruments MS2 susceptibility bridge. Cores CS03 and CS10 were measured using a MS2C sensor on half cores, core US01 using MS2E1 and core US02, using MS2F sensor, both along flat surface of half cores. The thermomagnetic behaviour of the bulk sediment sample from core US02, was determined on a horizontal force translation balance in air atmosphere in a magnetic field of 0.375 T and with a linear temperature increase.

3.3. Palynology

Samples were taken every 5 cm in the four cores. Initial processing of samples (1–2 ml) involved the addition of cold sodium pyrophosphate to deflocculate the sediment. Samples were then treated with cold hydrochloric acid (32%) and cold hydrofluoric acid (60%), followed by a further treatment with hydrochloric acid. The residual organic fraction was then screened through 125 and 10 μm mesh sieves and mounted on slides in glycerol. *Lycopodium* tablets were added at the beginning of the process for concentration estimates, which are provided in number of dinocysts per ml of wet sediment (c ml^{-1}).

The dinocysts were counted along side pollen and other microfossils. All palynomorphs appeared well preserved. The sum for percentages is made of all dinocysts. Varia are expressed as a percentage of the same sum as the other dinocysts. The percentages of the foraminiferal inner organic linings found in the palynological slides were displayed in the same way. A ratio pollen concentration on dinocyst concentration (P:D) has been determined according to McCarthy and Mudie (1998) in order to estimate the degree of continentality of the assemblage.

A statistical analysis available in Psimpoll (Bennett, 2007), the zonation by cluster analysis (CONISS) after square root transformation of the percentages, was applied. The zonation was calculated for the percentage diagrams.

The taxonomy of the few Caspian dinocyst species has been established by Marret et al. (2004) including three endemic species. Illustrations of Caspian dinocysts are also available in Leroy (2010) and Mudie et al. (2011). Three forms of *Lmac* have been defined: ss, A and B, in the KaraBogaz Gol; this is also used for the all the *Lmac* in the CS (Leroy et al., 2006). Form A has numerous, shorter (average 9 mm in length) and slender acuminate processes than form ss, with a small striated conical base (see plate 1–10 in Leroy (2010)). It is common in the KBG. Form B bears short (2–3 mm in length) bulbous and microgranulate processes with a typical large striated conical base (see plate III from 1 to 7 in Marret et al., 2004). It is common in the CS. For the CS, the length of the processes decreases from form ss to form B. The lengths of the CS processes (forms A and B) are generally short in comparison to the *Lmac* from the ocean (form ss), due to the lower salinities of the CS (Mertens et al., 2009).

In worldwide studies, Mertens et al. (2009) and Zonneveld et al. (2013) indicate that *Lmac* is restricted in surface sediment to temperate to equatorial regions. It can be found in a salinity range from at least 8.5 to 42 psu, and for temperature from 0 to 31 °C, specifically above 10 °C in summer and above 0 °C in winter. The former study established that longer processes are clearly developed at higher summer salinity, but are also somewhat related to temperature (Mertens et al., 2009, 2012). It is a coastal species and usually lives in regions in the vicinity of continental margins. It is frequent in highly stratified waters. However it is also present in areas with strong variability in trophic state such as caused by seasonal contrasts in upwelling cells and in river discharge plumes.

4. Results

4.1. The surface samples

The samples are organised by increasing percentage values of *Lmac* B from the top to the bottom of Fig. 3, except the bottom two samples which have high values of forms ss and A.

At the top of the diagram, the assemblages of the two lake samples (Almagol and Alagol) are composed only of *Brigantedinium* spp. At the bottom of the diagram, the dinocysts are dominated by *Lmac* B with increasing values of *Lmac* ss and often the presence of *Spiniferites belerius* (saline lagoons of BTork 1 and 2, and TR1). The bottom-most two samples are derived from hypersaline settings: the Aral Sea (AS17-5) and the Karabogaz Gol (KBG8-01) explaining respectively the abundance of *Lmac* ss and the high peak of *Lmac* A.

In the middle sample group, the spectra are dominated by *Impagidinium caspienense* and *Caspidinium rugosum rugosum*, with occasionally at the top end of the diagram the development of cysts of *Pentapharsodinium dalei* and *Spiniferites cruciformis*, respectively in north of the middle Caspian basin (cores US24 and US26) or more freshwater lagoons (Anzali).

4.2. Core sediment and dating

The sediment of **core US01**, off the coast of Turkmenistan, is silty with up to 20% clays. It has the highest amount of sand of the four cores, reaching 10–20% (Fig. 4). The core bottom has 4% organic matter, but this rapidly decreases upwards to 1%. The carbonate content is stable around 20%. The magnetic susceptibility is very low and increases upwards. Benthic foraminiferal tests are abundant (Appendix D).

The sediment of core **US02**, from the middle of the south basin, is clayey and silty with some sand from 8.5% at the base to 2% at the top. The organic matter progressively increases from 2 to 4%. This sequence has the highest content in carbonates of the four cores, reaching 30–40%. It is likely that some of the carbonate is derived from benthic ostracod valves as they are known in the top cm of this core (Boomer et al., 2005). The magnetic susceptibility is low. The Curie temperature for sample at 6 cm depth was 580 °C; the mineral carrying the magnetic susceptibility is magnetite (Fe_3O_4).

The sediment of core **CS03**, offshore from Anzali, is comprised of grey silts and clays with darker layers. The sediment is occasionally bioturbated by a network of animal tubes. The mean amounts of organic matter and carbonates are stable with respectively values of 3 and 17%. The magnetic susceptibility is low.

The sediment of core **CS10**, taken offshore from Babolsar, consists of clayey silts, sometimes with very fine sand, poorly sorted, getting darker with depth, ranging from dark grey to black with a reduced-sediment odour. Sediments are laminated through much of the sequence. Some part of the sequence appears burrowed (particularly the lower portion). The sequence has 3% of organic matter and 20% of carbonates as well as the highest magnetic susceptibility of the four cores.

The radionuclide results of core US02 have been published in Leroy et al. (2007). In brief the sedimentation rate obtained is 2.0 mm yr^{-1} for the top 22 cm of sediment. The base of the core is therefore estimated to be at AD 1709.

For core CS03, the record of artificial fallout radionuclides ^{241}Am and ^{137}Cs (Fig. 5) detected in the upper 104 cm of sediment displays a maximum at 83 cm depth that is assigned to the period of maximum weapons fallout, i.e. AD 1963 (Appleby, 2000). The corresponding averaged sedimentation rate is thus of 19 mm yr^{-1}. The radiometric ^{210}Pbexc profile (Fig. 5) does not display the regular exponential decrease with depth in the core as expected for a constant

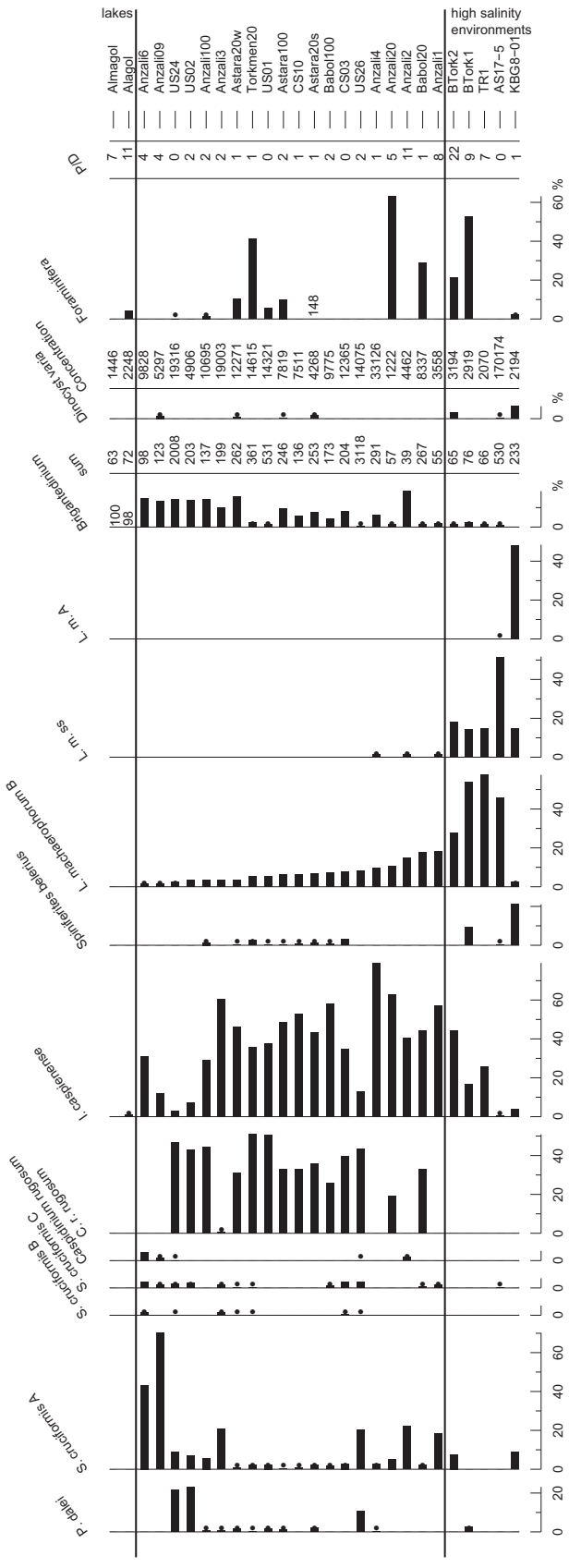

Fig. 3. Dinocyst assemblages from marine and lagoonal surface samples, mostly from the south basin of the Caspian Sea, topmost samples from two lakes and bottom-most samples from high salinity environments. Percentages are on the sum of all dinocysts. For the foraminiferal linings the sum includes all dinocysts except the foraminifera. Concentration in numbers of dinocysts per ml of wet sediment.

sedimentation rate. For the upper 63 cm, the profile nevertheless exhibits a roughly linear decreasing activity corresponding to a sedimentation rate of 20 mm yr^{-1} in good agreement with the artificial radionuclide results. Deeper in the core, the data are more scattered and would correspond to a higher sedimentation rate. Assuming that the sedimentation rate of the deeper part of the core is higher than 20 mm yr^{-1}, the age of the base of the core is estimated between AD 1963 and AD 1930. The use of other models (CIC, CRS, Appleby, 2000, and SIT, Carroll and Lerche, 2003) was not attempted because of the large discontinuities in the sampling depths. The sedimentation rate that was obtained, 20 mm yr^{-1}, is therefore exceptionally high and 10 times higher than that of core US02.

No dating is available for cores US01 and CS10. It is however likely that the sedimentation in front of the Babolsar River, for core CS10, will be similar or slightly lower than that of core CS03 because the Babolsar River (in front of the CS10 coring location) sediment discharge is minute when compared to that of the Sefidrud (a powerful river, but east of core CS03): 0.411 Mton yr^{-1} versus 26,000 Mton yr^{-1} (Lahijani et al., 2008).

4.3. Dinocysts in the four cores

In general the same range of taxa is found in the four cores (Fig. 6), with the usual dominance of *I. caspienense* and the abundance of *Lmac* under two forms: B and ss (Marret et al., 2004). *Pyxidinopsis psilata* has only rare occurrences.

4.3.1. Core US01, the shallow core off Turkmenistan

This sequence is largely dominated by only two taxa: *I. caspienense* whose percentages decrease slightly from 60 to 40%, and *Lmac* B whose percentages increase. *Lmac* ss and *S. belerius* have continuous curves. The P:D ratio is very low (if compared to modern samples, Fig. 3) indicating that more dinocysts than pollen are trapped in the sediment and therefore that the continental influence is low despite the proximity of the continent and that the dinocysts have found optimal conditions to grow. Foraminiferal linings have been found in significant numbers throughout the core and form a continuous curve.

4.3.2. Core US02, the last 300 years in the middle of the south basin

Zone US02-d1 has relatively high *S. cruciformis* values and a significant percentage of *C. rugosum*, not met in the surface samples. Zone US02-d2 has slightly less *S. cruciformis*, and after 10 cm much less *C. rugosum* and slightly more *Lmac* B.

The concentration is the lowest of the four cores due to the distance to the shores. The relatively low P:D displays an increasing overall trend. This diagram shows a mild trend to have opposite fluctuations of *P. dalei* cysts (highest values of the 4 cores) and *Lmac* B. This core overall shows assemblages that indicate the lowest salinities of the four cores. This is due to its location in a more open setting. No foraminiferal linings have been found in this sequence as the water depth is too great for the survival of these benthic organisms in the CS (Boomer et al., 2005).

4.3.3. Core CS03, the 20th century off Anzali

In zone CS03-d1, *I. caspienense* has maximal values, *P. dalei* cysts are well represented and the percentages of *Brigantedinium* are relatively high but decreasing. The concentration increases slowly across this zone while the P:D decreases upwards. In zone CS03-d2, *Lmac* B values are nearly twice as high as before. *P. dalei* cysts become rare. The concentration is clearly higher than in zone 1, while P:D is stable. This core shows a compelling opposition between *P. dalei* cysts and *Lmac* B.

The coring location, 15 km offshore, does not seem to be influenced by the freshwater outflow from the Anzali lagoon.

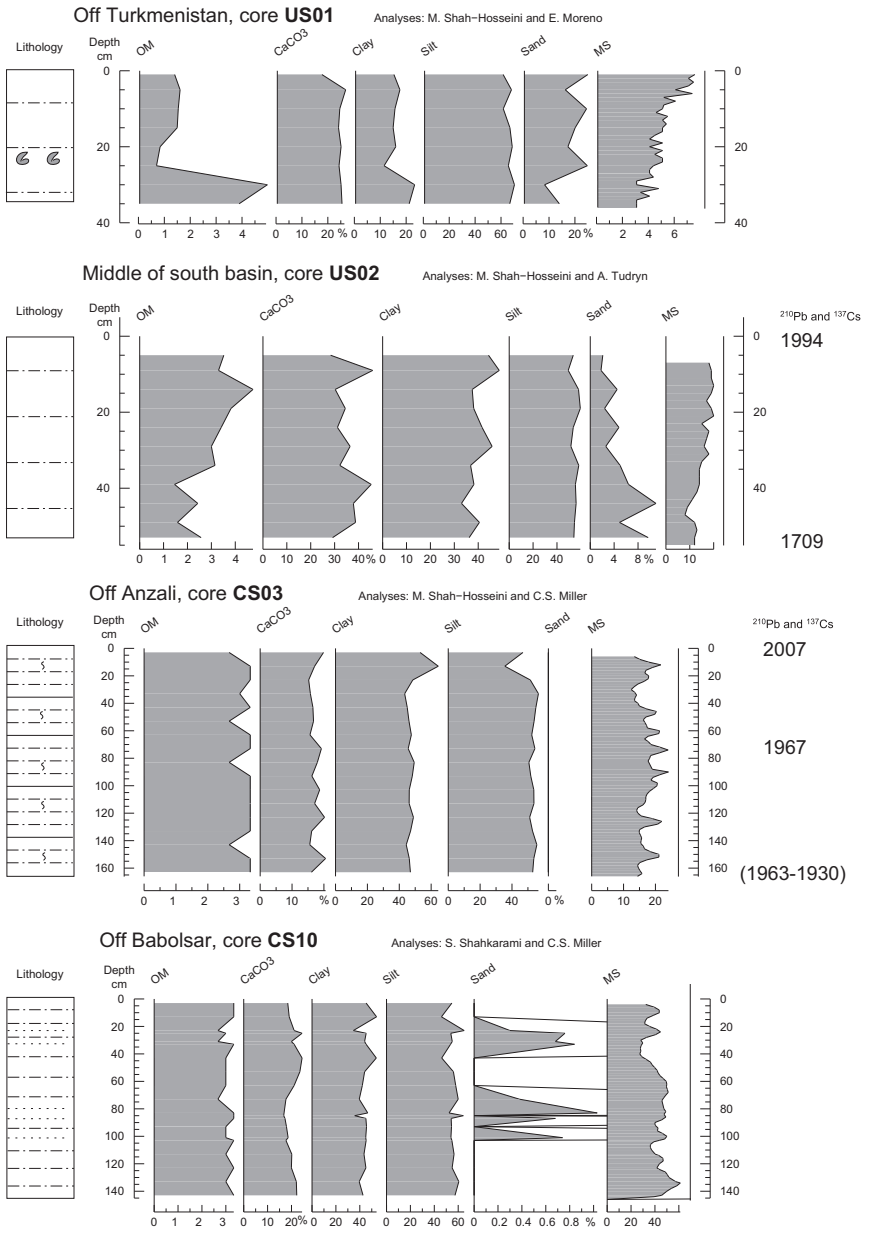

Fig. 4. Sedimentology of the four short cores: visual description of the lithology (dotted lines for sand, dash-dot lines for silt, horizontal lines for thin black layers, wiggles for bioturbation, and grey comas for shells), organic matter (OM) and calcium carbonate ($CaCO_3$) contents in percentages after Loss-On-Ignition, clay, silt and sand percentages by particle size analysis, as well as magnetic susceptibility (MS).

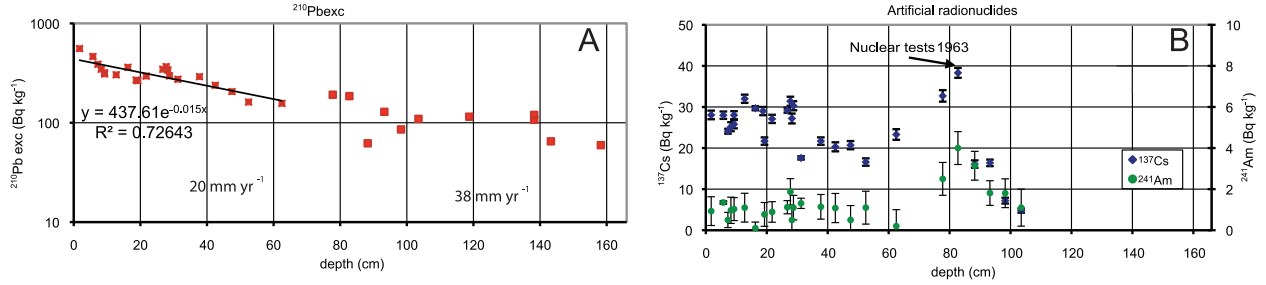

Fig. 5. Radionuclide dating of core CS03. (A): Profiles of $^{210}Pb_{exc}$.activities (Bq kg^{-1}, dry weight) with depth in cm. The regression line between the top and 65 cm depth corresponds to an average sedimentation rate of 2.0 cm yr^{-1}. Deeper in the core the regression line corresponds to 3.8 cm yr^{-1}. (B): Profiles of artificial radionuclides ^{137}Cs and ^{241}Am activities (fallout from nuclear weapon testing) with depth in cm. The maximum activity at 83 cm depth for both nuclides corresponds to the maximum global fallout peak in 1963. Vertical bars for error.

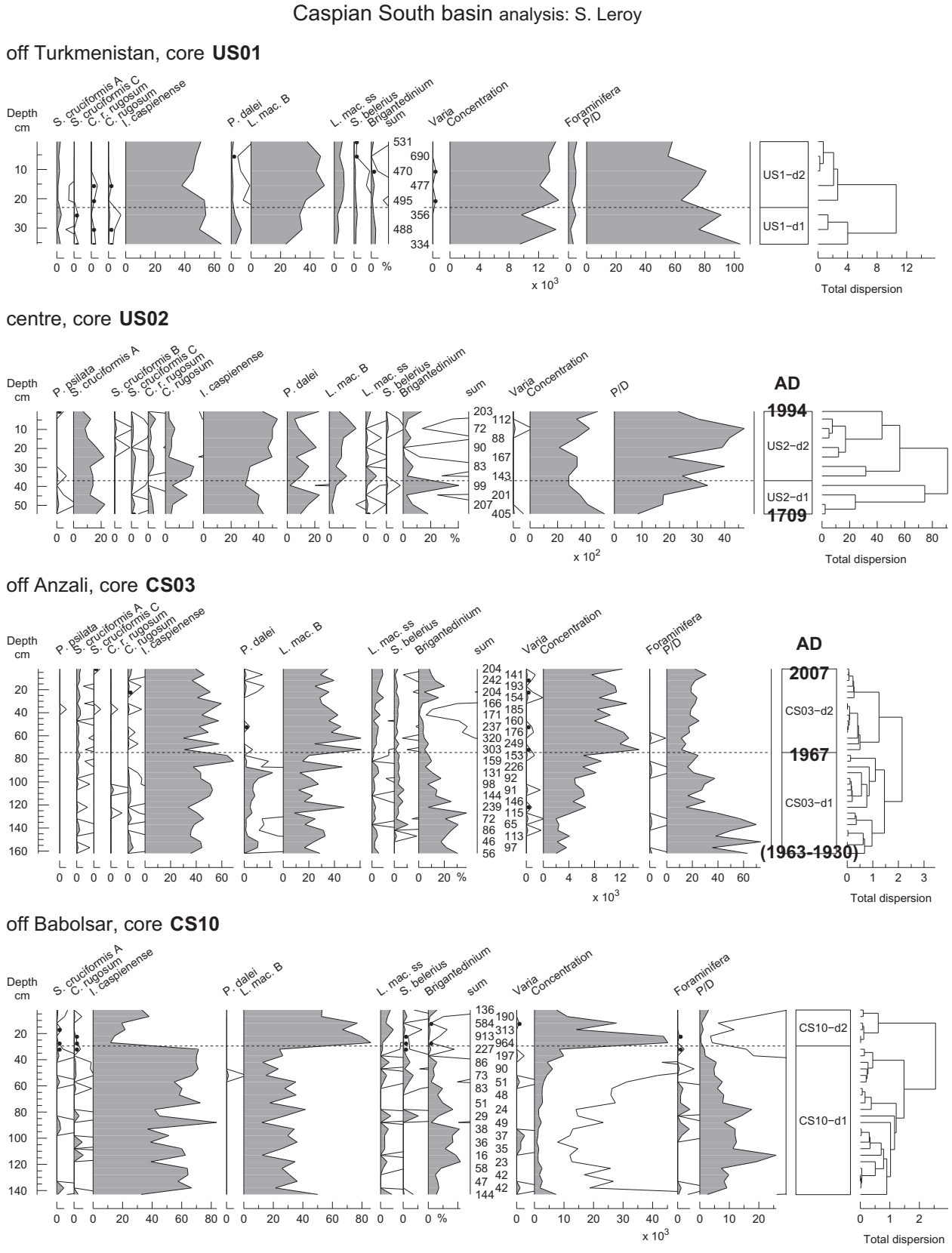

Fig. 6. Dinocyst diagrams of cores US01, US02, CS03 and CS10, taken in the south basin of the Caspian Sea. Concentration in numbers of dinocysts per ml of wet sediment. With 10× exaggeration curve. To the right dendrograms used for the zonation.

4.3.4. Core CS10, with massive dinocyst concentration increase off Babolsar

In zone CS10-d1, the values of *I. caspienense* are the highest of the four cores. The P:D is extremely high, showing a clear terrestrial influence similar to that in surface samples, e.g. in lakes (such as Alagol) and lagoons (Anzali and Bandar-e-Torkman).

In zone CS10-d2, after a sudden change, high percentages of *Lmac* B (80%) occur. These are also the highest values ever recorded in the CS. This occurs in parallel to a huge increase in the dinoflagellate cyst concentration.

The limit between zones CS03-d1 and d2 corresponds well to that between zones CS10-d1 and d2, with the same increase in *Lmac* B and ss percentages and in total concentration and the same decrease in *Brigantedinium* and in the P/D ratio. This change is well dated in core CS03 as it is just a few cm (75 cm) above the ^{237}Cs peak of AD 1963 at 83 cm, bringing the age of the limit at AD 1967.

4.4. Concentration of L. machaerophorum in thirteen Caspian Sea cores

In order to put in context the changes in *Lmac* observed in the four short cores, the records of *Lmac* concentrations in thirteen cores analysed by the same palynologist across the south and middle basins of the CS are compared (Fig. 7).

It is clear that the lagoons yielded the highest concentrations in *Lmac* often higher than 5000 cysts per ml of wet sediment (c ml^{-1}). Occasionally extraordinary values are even reached, such as at the top of the coastal core CS10 (>20,000 c ml^{-1}), at the base of the Anzali lagoon (HCGA05) and in the KaraBogaz-Gol (up to 141,000 c ml^{-1}). On the contrary, the cores taken in the middle of the basins display low values, even lower than 1000 c ml^{-1}, such as CP14 and US02 in the south basin and CP21 in the middle basin.

5. Discussion

5.1. Dinocyst distributions

The spectra from the surface sediment and the four cores are largely dominated by *I. caspienense* and *Lmac*. The near absence of *P. psilata* and the low values of *S. cruciformis* (for the latter, except the central core and some surface samples in the Lagoon of Anzali) are a characteristic of these four recent records and of the surface samples. *P. psilata* is mostly found in Khvalynian (Late Pleistocene) sediment (S. Leroy, unpublished data) and in lagoons and river deltas such as the Demchik area of the Lower Volga River (K. Richards, pers. comm.). This is easily explained both in terms of the higher salinity of the Neocaspian Sea and in terms of survival in lagoons where the salinity is variable and where the lagoons maintain at most times small areas of lower salinity if fed by rivers. The higher values of *S. cruciformis* in zone US02-d1 may reflect the much higher water levels of the LIA, which also have less saline waters as also seen in the lagoon of Anzali (Leroy et al., 2011).

The two southern cores have the highest percentages of *Brigantedinium*. This is explained by the proximity of a densely inhabited coastal area producing a lot of nutrients discharged into the sea.

The cosmopolitan species *P. dalei* cyst is clearly more abundant in the northern surface samples (samples US24 and 26), which are characterised by larger amplitudes of sea surface temperatures and the proximity of sea ice in winter (Marret et al., 2004).

On the one hand, based on the locations of the cores and the surface samples, it is possible to show that the three *Lmac* forms

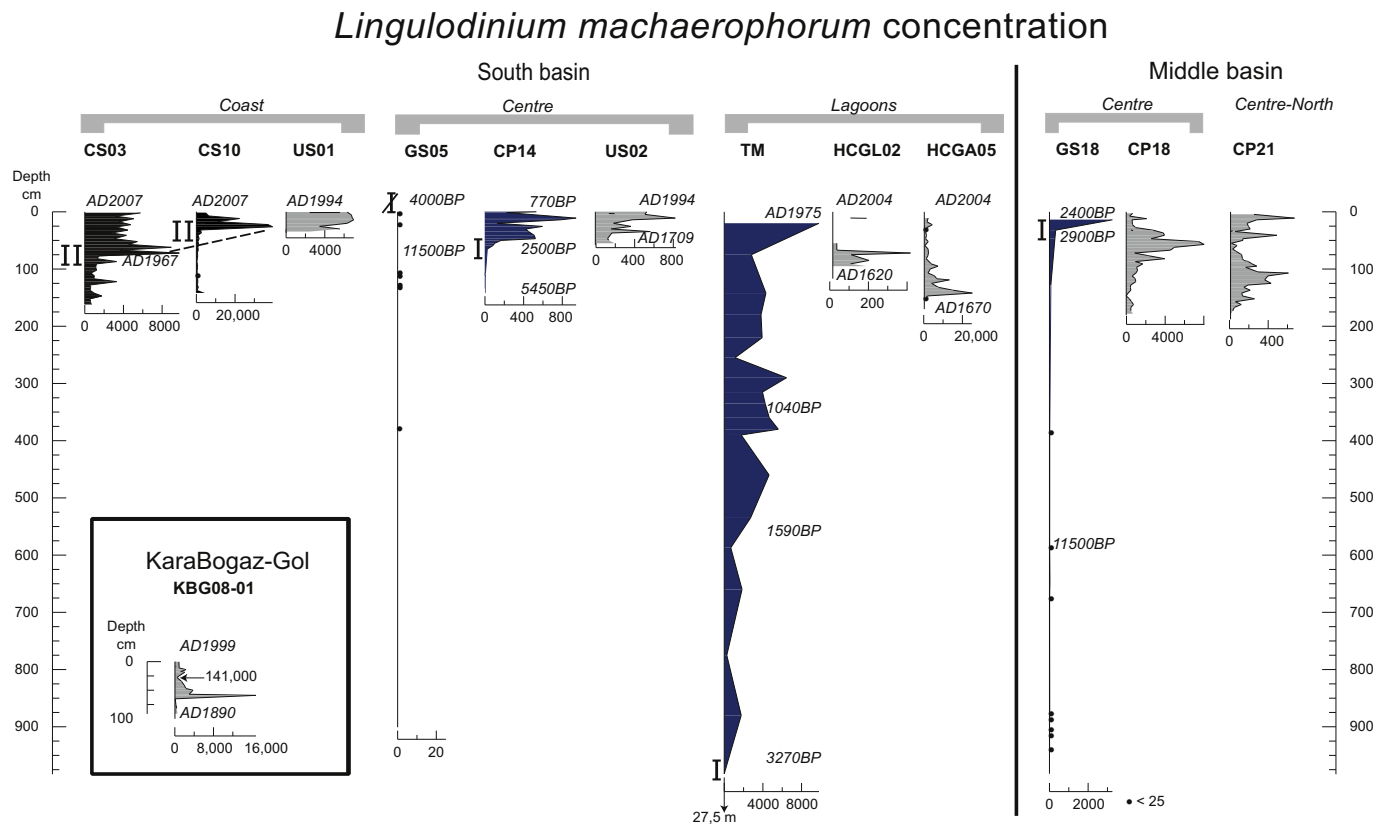

Fig. 7. *Lingulodinium machaerophorum* concentration in thirteen cores of the Caspian Sea over the last few millennia. The Roman number I indicates the first development of the *Lmac* in the CS, the Roman number II indicates the recent expansion. Core KBG08 (Leroy et al., 2006); cores GS05 and GS18 (Leroy, pers. comm.); Core TM (Leroy et al., 2013; the arrow indicates that only the part with *Lmac* in the 27.5 m long core is represented); cores HCGL02 and HCGA05 (Leroy et al., 2011); cores CP14, CP18 and CP21 (Leroy et al., 2007). Dates in AD or in calibrated years BP.

show an increasing salinity gradient from B, to ss and finally to A. On the other hand, *Lmac* percentages (all forms included) display an increase across the CS to the southeast, i.e. towards regions that are warmer and more saline. So the morphology of the cysts responds to the salinity (shown by another method in Mertens et al., 2009) but its biomass to temperature.

5.2. Exceptional sedimentation rate

The sedimentation rate of core US02, in the centre of the south basin, obtained by the radionuclide method is 2 mm per yr. This is 10 times higher than that obtained by radiocarbon on core CP14 taken close by Leroy et al. (2007). This difference could be caused not only by an expected lack of compaction of the top tens of cm of sediment in core US02 but also by a very recent (the last few centuries) increase of the sedimentation influx (Leroy et al., 2007). This radiocarbon-based value falls within the sedimentation rates of other cores from the deep basins, i.e. between 0.02 and 0.54 mm per yr (Amini et al., 2012).

The sedimentation rate in a short core (HCGA05, 170 cm long) from the Anzali Lagoon, is of 5 mm per year, that of core HCGL02 (95 cm long) in the lagoon of Amirkola is 2.5 mm per yr (Leroy et al., 2011), and that in cores from the Gorgan Bay is between 1.4 and 2.45 mm per yr (Karbassi and Amirnezhad, 2004). These values are higher than those from the core from the centre of the south basin. These lagoonal settings are indeed expected to have higher sedimentation rates than those of the open sea.

On the whole the values of the short cores are in the order of the sedimentation for the Cainozoic (Nadirov et al., 1997; Tagiyev et al., 1997).

However 20 mm per yr obtained on the coastal core CS03 is truly exceptional (Amini et al., 2012). This value is even higher than that of the Pliocene Productive Series (Kroonenberg et al., 2005). This is explained by the core location on the slope of the continental shelf. The time resolution of the palynological samples therefore reaches one sample every 2.5 years.

5.3. Shifts in L. machaerophorum concentration

This section focuses on what are the possible causes for the increase in *Lmac* visible in the four cores, more so for the two southern ones (Fig. 6 and marker II in Fig. 7). Moreover these increases of *Lmac* are often to the detriment of *P. dalei* cysts when present in the cores. The recent changes are then set in the context of the development of *Lmac* in the CS in the last few millennia (marker I in Fig. 7).

5.3.1. In the last decades

L. polyedrum, the motile form of *Lmac*, usually occurs in the water column during late summer, which suggests that a minimum temperature is needed for its development. *L. polyedrum* can bloom in nutrient rich and nutrient depleted waters: thus its distribution does not have to be restricted to areas with high nutrient concentrations in surface waters (Lewis and Hallett, 1997). Dinoflagellate biomass that shows a steep increase as part of anomalous algal blooms that occurred in the last few years in the CS are probably seen in the extreme dinocyst concentration increase across core CS10, especially since 1967 (marker II in Fig. 7). The causes for this are multiple, and are often attributed to nutrient washed into the sea by the rivers; however they may also be specifically linked to higher temperature and low wind conditions and therefore stratified waters (Soloviev, 2005; Nasrollahzadeh et al., 2011). A remote sensing analysis for the 2005 large-scale phytoplankton bloom indicated that an increase of 4 °C was observed in the bloom itself in comparison to surrounding waters. Low wind conditions and water stratification were also observed. In brief this would tend to indicate that *L. polyedrum* responds primarily to high temperatures, with salinity and nutrients as secondary factors.

In the 20th century, the water level has fluctuated by ±3 m a couple of times (Fig. 2A), but this seems to have been hardly registered in the fossil record (Fig. 6). More decisively, the sharp sea level rise between 1977 and 1995 has led to a salinity decrease. However *Lmac* percentages have strongly increased. Therefore this is more in line with the gradual increase of sea surface and air temperatures throughout this period (Fig. 2B–D).

5.3.2. In the Late Holocene

Successive dinocyst phases are characterised by the dominance of various dinocysts in the later part of the Late Pleistocene –Holocene history of the CS: 1) the most recent is a *Lmac* phase in the last few decades, 2) the next one is dominated by *I. caspienense* until c. 3.9 cal. ka ago, and 3) the oldest one, covering the early Holocene and Late Pleistocene, is dominated by *S. cruciformis* and *P. psilata*. This succession was already suspected in core CP14 (Leroy et al., 2007), but it is only with the additional cores US01, US02, CS03 and CS10 that the most recent phase became clearly visible.

The examination of thirteen records reveals the following history in the development of *Lmac* (Figs. 1 and 7). It is quasi absent from a 10 m long core in the centre of the south basin, core GS05, whose top reaches c. 4000 yr ago (Pierret et al., 2012; S. Leroy, unpublished data) and only present in the top cm of a 10 m long core in the centre of the middle basin, core GS18, from c. 2900 yr ago onwards (Boomer et al., 2005; S. Leroy, unpublished data) (marker I in Fig. 7). In the Holocene lagoonal core TM in Gomishan, SE of the south basin, *Lmac* starts to develop only from c. 3200 yr ago (Leroy et al., 2013). In the marine cores CP14, 18 and 21 covering most of the second half of the Holocene (Leroy et al., 2007), a steady increase is observed. More especially in core CP14, *Lmac* starts to develop c. 2500 yr ago (Leroy et al., 2007) (marker I in Fig. 7). The other much shorter records, KBG08, HCGL02 and HCGA05, show the abundance of this dinocyst in the last few centuries (Leroy et al., 2006, 2011). In core HCGA05 of the Anzali Lagoon (Leroy et al., 2011), *Lmac* fluctuates in anti-phase with *S. cruciformis*; this was interpreted as a salinity signal. The highest percentages of *Lmac* B, 80%, and *Lmac* A, 80%, are respectively found in core CS03 (Iranian coast) and in the Karabogaz-Gol.

Contrary to the CS, in the Black Sea, *Lmac* is already present at the beginning of the Holocene. In the SW of the Black Sea, *Lmac* occurs in cores M02-45 and MAR05-13 respectively over the last 9500 uncal. ^{14}C years and 11,000 uncal. ^{14}C years (Marret et al., 2009; Bradley et al., 2012) (note that the Black Sea radiocarbon dates are often uncalibrated and uncorrected for the reservoir effect due to major uncertainties). From 6 uncal. ^{14}C ka, it is even largely dominant. It peaks from 6 to 5 uncal. ^{14}C ka, which is considered the warmest period in the climate of the Black Sea region. The topmost part of the core estimated to be close to the present shows at least 80% of *Lmac* ss. Marret et al. (2009) suggested that these high values were due to anomalous blooms of this species.

In a Black Sea sedimentary sequence, Verleye et al. (2009) found an opposition, similar to that of the present study, between *Lmac* and *P. dalei* cysts interpreted here as less river input versus higher terrigenous input. In the Sea of Barents, the abundance of cysts of *P. dalei* increases according to Voronina et al. (2001) near high productivity waters. An investigation of dinocysts in a core from the Marmara Sea covering the Late Pleistocene and Holocene considers *Lmac* as a thermophilous taxon (Londeix et al., 2009).

Lmac is present with strong percentages shifts in the 2000 yr-long record obtained from the Aral Sea (Sorrel et al., 2006). Although the authors suggest that the salinity is the first forcing factor, they recognise that the temperature in the Tien Shan Mountains (by control on snow melt) are the ultimate driver.

In brief in the CS, contrary to the Black Sea, it appears that the *Lmac* development started slowly only c. 3200 yr ago (marker I in Fig. 7) and has strongly accelerated in the last decades (marker II in Fig. 7).

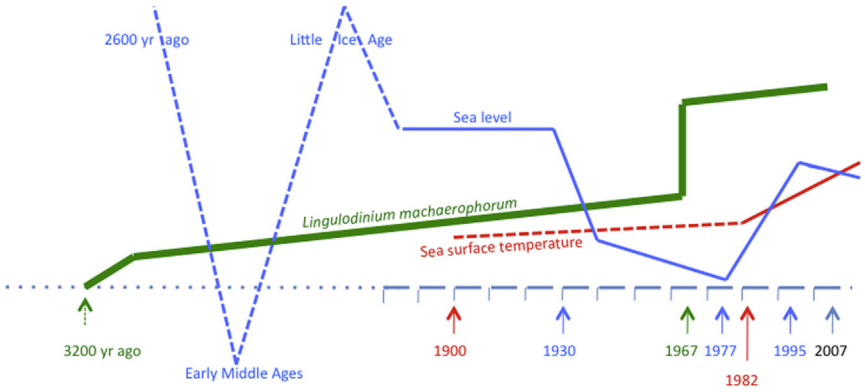

Fig. 8. Outline of the main changes in the last millennia. The green bold line shows the abundance of the *Lingulodinium machaerophorum* over the last 3200 years (see Fig. 7). The blue curve is a rough synthesis of sea levels since the highstand of 2600 years ago (Kroonenberg et al., 2007; Naderi Beni et al., 2013a,b) (dashed) and observed levels (continuous line; Leroy et al., 2006). The red curve is sea surface temperature from discontinuous observations (dashed line) and from instrumental data and satellite observations (continuous curve) (Ginzburg et al., 2005). Note the change in the horizontal axis scale, which reflects time. The vertical scale is arbitrary and only shows an outline of the changes. (For interpretation of the references to colour in this figure legend, the reader is referred to the web version of this article.)

5.3.3. Possible causes

The causes for the development of *Lmac* in the CS c. 3200 yr ago could be linked to the instauration of favourable regional conditions, a possible long-term recovery from glacial meltwater inflow (Leroy et al., 2007) or at a global level. It is not an appearance as the species was already found in extremely low numbers in the CS in the Holocene (cores GS05 and GS18), as well as in the Late Khazarian in Tsagan-Aman (Tudryn et al., 2012) and in the Pliocene (K. Richards, pers. comm.).

Changes in phytoplankton abundance may be driven by several factors that may confound the climatic signal (Adrian et al., 2009). In the present situation, it is however possible to eliminate two important factors that may have explained the changes in *Lmac*: sea level changes linked to salinity and eutrophication. The causes of the second and more recent development of *Lmac* are not sea levels that have fluctuated widely during that time period. During the LIA, the water level was 6 m higher than at present (palaeoenvironmental, archaeological and documentary evidences; Brückner, 1890; Leroy et al., 2011; Naderi et al., 2013a). During the early Middle Ages, the water levels were lower by 2–4 m as attested by the numerous walls built by the Sasanian Empire (archaeological and documentary evidences in Brückner, 1890; Omrani Rekavandi et al., 2007). A highstand similar to the LIA has been recorded between 2600 and 2300 cal. yr BP (sediment: Kroonenberg et al., 2007; Kakroodi et al., 2012; Naderi et al., 2013a,b). These significant changes have so far not been recorded in the *Lmac* curve. So sea level changes have taken place in the last millennia and even centuries but did not significantly affect the percentages of *Lmac*. In addition, because the shift to increased values of *Lmac* is older than anthropogenic eutrophication and because here *Lmac* is inversely correlated to *P. dalei*, eutrophication may be secondary only in explaining the CS trend. Moreover it is only the coasts of the CS that are becoming mesoeutrophic, and especially since 2001 (Dumont, 1998; Nezlin, 2005).

The temperature trend across the later part of the Holocene, due to a long-term recovery from the end of the meltwater inflow into the CS, is the initial forcing factor. The recent global warming trend detected in the CS 20th century instrumental data (air and sea surface), and confirmed for the first decade of the 21st century (Fig. 2B–D), has fuelled the second increase of *Lmac*.

In brief (Fig. 8), it has been shown that the increases of *Lmac* 1) some 3200 years ago was due to natural global and/or regional climatic forcing working, such as a long-term recovery from meltwater inflow, and 2) in the last decades was due to recent warming of the surface waters related to a recent anthropogenic-induced global forcing. It is therefore hypothesised that the temperature increase is the primary forcing factor, and salinity increase is just a corollary, reinforced by the closed basin setting.

6. Conclusions

This study is the first to provide an analysis of modern and very recent dinocyst assemblages for the CS, with more details for the south basin in some cores with exceptional sedimentation rates.

This investigation of surface samples has provided a baseline for the present state of the CS and surroundings, with the dinocysts reflecting surface water parameters. This may serve as a reference when comparing it with past states and future ones. More specifically for the present, the following was observed: more *P. dalei* cysts in the north at proximity to winter sea ice and with larger seasonal contrasts, more *S. cruciformis* in freshwater lagoons or in the oligohaline north, and more *Lmac* in the warmer south and in higher salinity settings.

New analyses on four short cores in the CS (with one of them with a sedimentation rate of 20 mm per year) have shown a recent expansion of the dinoflagellate cyst *Lmac*. When these results are placed in the context of thirteen sequences in the CS, a robust signal is obtained: the dinocyst concentration trend is the end result of a natural increase that has started slightly over three millennia ago. The overall trend has recently been amplified by global warming as shown by instrumental data. This warming (and the subsequent stratification increased) has significantly changed the dinocyst assemblage in terms of relative abundances and in terms of concentration; whereas salinity via sea level changes, which are typical driving factors of this species abundance, were shown here in the Caspian Sea not to have had a significant influence.

The dinocyst assemblages and the sea surface temperatures indicate that the CS has moved into the Anthropocene, i.e. the post-industrialisation period (Crutzen, 2002), as many other lakes (Adrian et al., 2009). The CS is a fragile ecosystem exploited by multiple users who each wish to sustain their economical development and who will have to change in order to adapt to the present changes.

The next steps could be 1) to make culture experiments on the effect of temperature on abundance of *Lmac* (e.g. Hallett, 1999), and 2) to measure the lengths of the *Lmac* processes in the CS as in the Black Sea (Mertens et al., 2009, 2012). Both would lead to the establishment of quantitative reconstructions of environmental parameters such as temperature and salinity in the Caspian Sea over the Holocene and longer time periods.

Acknowledgements

Our gratitude goes to F. Gasse, the leader of the project “Understanding the Caspian Sea erratic fluctuations”, European

Contract INCO-Copernicus no. IC15-CT96-0112, to F. Guichard and P. Tucholka for collection of Usnel box cores, to P.J. Giannesini and E. Moreno, past and present curators of cores from the Caspian Sea (Laboratoire de Géologie, Museum d'Histoire Naturelle de Paris, France). The Golestan samples were kindly provided by A. Kakroodi. All the palynological samples were treated at Brunel University by C. Miller, who also made the magnetic susceptibility measurements of the two Kajak cores. This article is a contribution to the European project Marie Curie, CLIMSEAS-PIRSES-GA-2009-247512: "Climate Change and Inland Seas: Phenomena, Feedback and Uncertainties. The Physical Science Basis". S. Kershaw and L. López-Merino (Brunel University) have provided critical feedback on earlier versions of the manuscript. M. Turner (Brunel University) has kindly revised the English of the manuscript.

Appendices

Appendix A. Modern oceanographic parameters for Anzali and Babolsar

Offshore from Anzali (one of the four main studied locations, S–SW Caspian coast of Iran, Fig. 1) across the four seasons of the year 2006, the temperature and salinity profiles at a station with 50 m water depth indicate a constant temperature down to 30 m followed by a thermocline (26–9 °C). The salinity (9.32 and 12.25) is also constant, with just a drop in surface waters in February (Bagheri et al., 2011).

The temperature structure offshore from Babolsar (close to another one of the four main studied locations, S–SE Caspian coast of Iran, Fig. 1) is characterised by a strong seasonal thermocline, located between 20 and 50 m depth with a 15 °C temperature difference across it in summer. In autumn, the thermocline gradually weakens and, at the end of winter, it disappears before its reformation in the early spring. The salinity is 12 psu with a slight decrease to 11 psu in enhanced river flow to the sea (Zaker et al., 2007, 2011).

Temperature and salinity measurements along the Iranian coast show similar temperatures but with slightly wider seasonal amplitude in the west (Appendix B). The salinity increases eastwards because of the inflow of freshwater in the west via Anzali lagoon and the Sefidrud River.

No sewage control exists in Babolsar: industrial, domestic and agricultural wastes go to the sea via the river. Moreover, in both the flat coastal plains of Anzali-Rasht and Babolsar, a significant source of nutrients is derived from the fertilizers used in the rice fields.

Appendix B

Table B1
Location of surface samples for dinocysts according to increasing values of *L. machaerophorum* B.

Label	Lat N	Long E	Water depth in m	Location brief description	Sampling date	Type of sample	Surface temperature in C	Surface salinity	Date of measurements & source	Published palynological sample label
Almagol	37 25 53.50	54 38 52.18	0.6	Core top in Modern Lagoon, water at zero	Sept. 2010	Lagoon	11–28	2–3	Not measured at sampling; Patimar (2008) for 2000–2002	
Alagol	37 21 59.48	54 34 44.33	0.6	Core top in Modern Lagoon, water at −6 m	Sept. 2010	Lagoon	10–27	3.5–4.0	Not measured at sampling; Patimar (2008) for 2000–2002	
Anzali 09	37 26 56.6	49 22 49.8	1.8	Grab HCGA09, 280 m away	26 June 2008	Lagoon	n/a	n/a	Not measured at sampling	
Anzali 6	37 25 1.94	49 25 17.93	1–2	Grab Anzali Lagoon surface	1995	Lagoon	4.5–27.5	0.8–3.0	Not measured at sampling; but across 2000[a]	Ens8[a]
US24	43 19 14	49 06 02	61	Core top	Aug. 1994	Marine	25.5	9.5	F. Chalié, snapshot	
US02	39 16	51 28	315	Core top, SR9406US14, SR01US9402, at 0.5 cm depth	Aug. 1994	Marine	24.7	10.9	F. Chalié, snapshot	US02[b]
Anzali 3	37 29 5.62	49 19 14.05	1–2	Grab Anzali Lagoon surface	1995	Lagoon	4.5–27.5	0.5–4.5	Not measured at sampling; but across 2000[a]	Ens15[a]
Anzali 100	37 36	49 32	100	Grab during phytoplankton survey	Jan. 2011	Marine	9.3–30	7–11	H. S. Nasrollahzadeh, annual	
Astara 20W	38 24	49 01	20	Grab during phytoplankton survey	Winter 2010	Marine	7.5–33	7.5–14	H. S. Nasrollahzadeh, annual	
Torkman 20	37 05	53 35	20	Grab during phytoplankton survey	Winter 2010	Marine	n/a–29.5	9–10	H. S. Nasrollahzadeh, annual	
US01	38 44 10	53 11 15	13	Core top, SR9403US09, SR01US9401, at 0.5 cm depth	Aug. 1994	Marine	28	10.5	F. Chalié, snapshot	
CS10	36 48 25.0	52 33 02.8	250	Core top, core CS10 at 2 cm	2007	Marine	18	12	Not measured at sampling, but snapshot for a station with 42 m water depth in Nov. 2008 (Jamshidi & BinAbuBakar, 2011)	
Astara 100	38 22	49 08	100	Grab during phytoplankton survey	Summer 2010	Marine	7.8–32.4	7–12	H. S. Nasrollahzadeh, annual	
Astara 20S	38 24	49 01	20	Grab during phytoplankton survey	Summer 2010	Marine	7.5–32.6	7.5–14	H. S. Nasrollahzadeh, annual	
Babol 100	36 49	52 39	100	Grab during phytoplankton survey	Jan. 2011	Marine	9.6–28	9.5–13	H. S. Nasrollahzadeh, annual	
US26	43 19 36	49 05 58	61	Core top	Aug. 1994	Marine	25.5	9.5	F. Chalié, snapshot	

Table B1 (*continued*)

Label	Lat N	Long E	Water depth in m	Location brief description	Sampling date	Type of sample	Surface temperature in C	Surface salinity	Date of measurements & source	Published palynological sample label
CS03	37 35 28.3	49 34 16.6	250	Core top, core CS03 at 2 cm	2007	Marine	10	12	Not measured at sampling, but for a station nearby in 2008 (Ghaffari et al., 2010; S. Haghani)	
Anzali 4	37 25 18.16	49 26 48.36	1–2	Grab Anzali Lagoon surface	1995	Lagoon	4.5–27.5	1.0–5.0	Not measured at sampling; but across 2000[a]	Ens6[a]
Anzali 20	37 30	49 29	20	Grab during phytoplankton survey	Jan. 2011	Marine	7–32	7–10	H. S. Nasrollahzadeh, annual	
Anzali 2	37 27 40.01	49 22 11.41	1–2	Grab Anzali Lagoon surface	1995	Lagoon	4.5–27.5	0.5–1.0	Not measured at sampling; but across 2000[a]	Ens12[a]
Babol 20	36 46	52 40	20	Grab during phytoplankton survey	Jan. 2011	Marine	10–29.4	8–11.4	H. S. Nasrollahzadeh, annual	
Anzali 1	37 24 55.24	49 29 9.12	1–2	Grab Anzali Lagoon surface	1995	Lagoon	4.5–27.5	0.6–2.0	Not measured at sampling; but across 2000[a]	Ens1[a]
BTorkman 2	36 53 57.3	54 02 46.1	0.1	Artificial pool behind bay, salinity 22, reeds, *Salicornia*	20 May 2011	Lagoon	n/a	22	S. Leroy, snapshot	
BTorkman 1	36 53 49.7	54 02 39.4	0.1	Harbour, salinity 17, mud with *Salicornia* meadow	20 May 2011	Lagoon	n/a	17	S. Leroy, snapshot	
TR1	37 03 43.70	54 01 59.02	0.1	Core top in Modern Lagoon, water at −28 m, Gm1short	Sept. 2010	Lagoon	9–30	20–24	Spring–Summer in 2007 (Patimar et al., 2009)	
AS17	46 31 04	60 41 55	12.5	Core top, AS17-5 at 0.5 cm	17 June 1999	Marine	n/a	22	(Boomer et al., 2003; S. Juggins pers. comm.) snapshot	AS0.5[b]
KBG08-01	41 51	53 15	0.8	Core top, KBG08-01 at 0.5 cm depth	1999	Marine	−3.5 to +33	170–250	1999[b]	KBG08-01[b]

n/a: not available.
[a] Kazancı et al., 2004.
[b] Leroy et al., 2006.

Appendix C. Core numbering and location. Note: Locations and water depths for the two Usnel cores are approximate owing to poor weather conditions and navigation tool performances.

Full name General location	Short name	Length in cm	Latitude N Longitude E	Water depth in m	Date corer
On board no SR9403US09 Museum no SR01US9401 Offshore Turkmenistan	US01	36	38°44′10″ 53°11′15″	13	1994 Usnel box
On board no SR9406US14 Museum no SR01US9402 Centre of south basin	US02	57	39°16′ 51°28′	315	1994 Usnel box
CS07-03 Offshore Anzali	CS03	166	37°35′28.3″ 49°34′16.6″	250	2007 Kajak
CS07-10 Offshore Babolsar	CS10	147	36°48′25.0″ 52°33′02.8″	250	2007 Kajak

Appendix D. The analysis of foraminiferal tests in core US01

Materials and methods

Due to the continuous presence of foraminiferal linings in palynological slides, core US01 was selected for foraminiferal test analyses. Seven samples were taken at approximately 5 cm intervals. The samples were dried at 50 °C in an oven and weighed. Subsequently the samples were treated with a 4% solution of H_2O_2 for 15 h and were wet sieved through mesh sizes of 53, 63, 125, 250 μm and then were dried again. Afterwards, all foraminifera were picked and identified from 53, 63, 125 and 250 μm fractions under a binocular microscope and finally percentages were calculated for each species. In the case of samples rich in foraminifera, the samples were split into 1/8 prior to sieving, then picked and the total abundances were then calculated by multiplying.

The taxonomic classification followed the suprageneric taxonomy of Loeblich and Tappan (1987), with some information from Birshtein et al. (1968).

Results

The sediment contains five different euryhaline benthic foraminifera taxa: *Ammonia beccarii* (47–87%), *Elphidium littorale* (also known as *Elphidium littorale caspicum*, *Retroelphidium littorale*, *Retroelphidium caspicum*, *Elphidium caspicum caspicum* and *E. gunteri*) (10–52%), *Elphidium shochinae* (0.9–0.83%), *Elphidiella brotzkajae* (0.6–4.87%) and *Cornuspira* sp. (0.11%) (Fig. D1). *A. beccarii* is the most abundant taxon in this core and *Elphidium shochinae* and *Cornuspira* sp. are the rarest.

The comparison of foraminiferal abundance between the four fractions shows a maximum abundance in the 63–125 and 125–250 μm fractions. The maximal abundance of foraminifera is at 24 cm depth, with assemblages displaying a dominance by *A. beccarii*. The lowest foraminiferal concentration is recorded at 7 cm depth (Fig. D1). In the entire core, *A. beccarii* maximum abundance is at 14 cm depth and minimum abundance at the 34 cm of core, but the abundance of *E. littorale* is reversed at these depths.

The core US01 is characterised by silty sediments with sand and clay with low organic matter except below 27 cm depth where it reaches 5%. *A. beccarii* dominates this core and is indicative of a shallow-marine environment with sandy bottom (Sgarrella and Moncharmont Zei, 1993). However below 20 cm depth, *Elphidium littorale* is more abundant and this could be parallelled to the higher organic matter values.

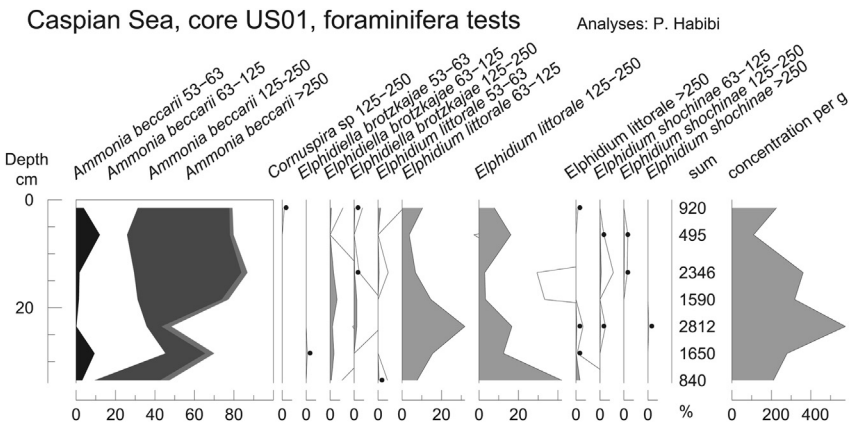

Fig. D1. Foraminiferal assemblages of core US01, taken in the south basin of the Caspian Sea. Names with fraction size in μm.

References

Adrian, R., O'Reilly, C.M., Zagarese, H., Baines, S.B., Hessen, D.O., Keller, W., Livingstone, D.M., Sommaruga, R., Straile, D., Van Donk, E., Weyhenmeyer, G.A., Winder, M., 2009. Lakes as sentinels of climate change. Limnology Oceanography 54 (6), 2283–2297.

Amini, A., Moussavi Harami, R., Lahijani, H., Mahboubi, A., 2012. Holocene sedimentation rate in Gorgan Bay and adjacent coasts in southeast of Caspian Sea. Journal of Basic and Applied Scientific Research 2 (1), 289–297.

Appleby, P.G., 2000. Radiometric dating of sediment records in European mountain lakes. Journal of Limnology 59 (Suppl. 1), 1–14.

Arpe, K., Leroy, S.A.G., 2007. The Caspian Sea Level forced by the atmospheric circulation as observed and modeled. Quaternary International 173–174, 144–152.

Arpe, K., Bengtsson, L., Golitsyn, G.S., Mokhov, I.I., Semenov, V.A., Sporyshev, P.V., 2000. Connection between Caspian Sea level variability and ENSO. Geophysical Research Letters 27, 2693–2696.

Arpe, K., Leroy, S.A.G., Lahijani, H., Khan, V., 2012. Impact of the European Russia drought in 2010 on the Caspian Sea level. Hydrology and Earth System Science 16, 19–27. http://dx.doi.org/10.5194/hess-16-19-2012.

Bagheri, S., Mansor, M., Makaremi, M., Sabkara, J., Wan Maznah, W.O., Mirzajani, A., Khodaparast, S.H., Negarestan, H., Ghandi, A., Khalilpour, A., 2011. Fluctuations of phytoplankton community in the coastal waters of Caspian Sea in 2006. American Journal of Applied Sciences 8 (12), 1328–1336.

Bagheri, S., Mansor, M., Turkoglu, M., Marzieh, M., W.O., Wan Maznah., Negaresatan, H., 2012. Phytoplankton composition and abundance in the Southwestern Caspian Sea. Ekoloji 21, 32–43.

Bennett, K., 2007. Psimpoll and Pscomb Programs for Plotting and Analysis. Version Psimpoll 4.27. http://chrono.qub.ac.uk/psimpoll/psimpoll.html (Last accessed 09.03.13.).

Birshtein, Y.A., Vinogradov, L.G., Kondakov, N.N., Astakhova, M.S., Romanova, N.N. (Eds.), 1968. Atlas of Invertebrates of the Caspian Sea. Pishchevaya Promyshlennost, Moscow (in Russian).

Boomer, I., Hoorne, D., Slipper, I.J., 2003. The use of ostracods in palaeoenvironmental studies, or what can you do with an ostracod shell? Paleontological Society Papers 9, 153–179.

Boomer, I., von Grafenstein, U., Guichard, F., Bieda, S., 2005. Modern and Holocene sublittoral ostracod assemblages (Crustacea) from the Caspian Sea: a unique brackish, deep-water environment. Palaeogeography, Palaeoclimatology, Palaeoecology 225 (1–4), 173–186.

Bradley, L., Marret, F., Mudie, P., Aksu, A., Hiscott, R., 2012. Constraining Holocene sea-surface conditions in the southwestern Black Sea using dinoflagellate cysts. Journal of Quaternary Science 27 (8), 835–843.

Brückner, E., 1890. Klima-Schwankungen seit 1700 nebst Bemerkungen über die Klimaschwankungen der Diluvialzeit. In: Geographische Abhandlungen herausgegeben von Prof. Dr Albrecht Penck, E. Hölzel, Vienna and Olmütz, vol. IV (2), pp. 153–484.

Carroll, J., Lerche, I., 2003. Sedimentary Processes: Quantification Using Radionuclides. Elsevier, Oxford.

Cazenave, A., Bonnefond, K., Dominh, K., Schaeffer, P., 1997. Caspian sea level from Topex-Poseidon altimetry: level now falling. Geophysical Research Letters 24, 881–884.

Climatic Research Unit, University of East Anglia, no date, http://www.cru.uea.ac.uk/cru/data/temperature/crutem4/station-data.htm (last accessed 09.03.13.).

Crétaux, J.-F., Birkett, C., 2006. Lake studies from satellite radar altimetry. Comptes Rendus Geoscience 338, 1098–1112.

Crutzen, P.J., 2002. Geology of Mankind. Nature 415, 23.

Dean Jr., W.E., 1974. Determination of carbonate and organic matter in calcareous sediments and sedimentary rocks by loss on ignition: comparison with other methods. Journal of Sedimentary Geology 44, 242–248.

Dee, D.P., et al., 2011. The ERA-Interim reanalysis: configuration and performance of the data assimilation system. Quarterly Journal of the Royal Meteorological Society 137 (656), 553–597. http://dx.doi.org/10.1002/qj.828. Part A.

Deflandre, G., Cookson, I.C., 1955. Fossil microplankton from Australia late Mesozoic and Tertiary sediments. Australian Journal of Marine and Freshwater Research 6, 242–313.

Dumont, H.J., 1998. The Caspian Lake: history, biota, structure, and function. Limnology and Oceanography 43 (1), 44–52.

Einsele, G., Hinderer, M., 1997. Terrestrial yield and the lifetimes of reservoirs, lakes and larger basins. Geologische Rundschau 86, 288–310.

Ghaffari, P., Lahijani, H.A., Azizpour, J., 2010. Snapshot observation of the physical structure and stratification in deep-water of the South Caspian Sea (western part). Ocean Science 6, 877–885.

Ginzburg, A.I., Kostianoy, A.G., Sheremet, N.A., 2005. Sea surface temperature variability. In: Kostianoy, A., Kosarev, A. (Eds.), The Caspian Sea Environment. Springer, Berlin Heidelberg, pp. 59–81.

Golitsyn, G.S., Panin, G.N., 1989. The water balance and modern variations of the level of the Caspian Sea. Soviet Meteorology and Hydrology (English Translation) 1, 46–52.

Hallett, R.I., 1999. Consequences of Environmental Change on the Growth and Morphology of *Lingulodinium polyedrum* (Dinophyceae) in Culture. Doctor of Philosophy thesis. University of Westminster, UK.

Howard, M.D.A., Smith, G.J., Kudela, R.M., 2009. Phylogenetic relationships of Yessotoxin-producing dinoflagellates, based on the large subunit and internal transcribed spacer ribosomal DNA domains. Applied and Environmental Microbiology 75 (1), 54–63.

Jamshidi, S., BinAbuBakar, N., 2011. Oceanographic study in coastal waters in Babolsar. Asian Journal of Earth Sciences 4 (1), 1–8.

Kakroodi, A.A., Kroonenberg, S.B., Hoogendoorn, R.M., Mohammadkhani, H., Yamani, M., Ghasssemi, M.R., Lahijani, H.A.K., 2012. Rapid Holocene sea-level changes along the Iranian Caspian coast. Quaternary International 263, 93–103.

Karbassi, A.R., Amirnezhad, R., 2004. Geochemistry of heavy metals and sedimentation rate in a bay adjacent to the Caspian Sea. International Journal of Environmental Science & Technology 1 (3), 191–198.

Kavak, M.T., 2012. Long term investigation of SST regime variability and its relationship with phytoplankton in the Caspian Sea using remotely sensed AVHRR and SeaWiFS data. Turkish Journal of Fisheries and Aquatic Sciences 12, 709–717.

Kazancı, N., Gulbabazadeh, T., Leroy, S.A.G., Ileri, O., 2004. Sedimentary and environmental characteristics of the Gilan-Mazenderan plain, northern Iran: influence of long- and short-term Caspian water level fluctuations on geomorphology. Journal of Marine Systems 46 (1–4), 145–168.

Khrustalyov, Y.P., Artiukhin, Y.V., 1992. Sedimentation in the southern inland seas of the arid zone of the USSR. Marine Geology 103, 503–512.

Kideys, A.E., Roohi, A., Eker-Develi, E., Mélin, F., Beare, D., 2008. Increased chlorophyll levels in the Southern Caspian Sea following an invasion of Jellyfish. Research Letters in Ecology. Article ID 185642.

Kosarev, A.N., 2005. Physico-geographical conditions of the Caspian Sea. In: Hutzinger, O. (Ed.), The Handbook of Environmental Chemistry, Water Pollution, Part P, vol. 5. Springer, Berlin, pp. 5–31.

Kosarev, A.N., Yablonskaya, E.A., 1994. The Caspian Sea. SPB Academic Publishing, The Hague, p. 259.

Kouraev, A.V., Papa, F., Mognard, N.M., Buharizin, P.I., Cazenave, A., Cretaux, J.-F., Dozortseva, J., Remy, F., 2004. Sea ice cover in the Caspian and Aral Seas from historical and satellite data. Journal of Marine Systems 47, 89–100.

Kroonenberg, S.B., Simmons, M.D., Alekseevski, N.I., Aliyeva, E., Allen, M.B., Aybulatov, D.N., Baba-Zadeh, A., Badyukova, E.N., Davies, C.E., Hinds, D.J., Hoogendoorn, R.M., Huseynov, D., Ibrahimov, B., Mamedov, P., Overeem, I., Rusakov, G.V., Suleymanova, S., Svitoch, A.A., Vincent, S.J., 2005. Two Deltas, Two Basins, One River, One Sea: the Modern Volga Delta as an Analogue of the Neogene Productive Series, South Caspian Basin. River Deltas – Concepts,

Models, and Examples. In: SEPM Special Publication No. 83. SEPM, Society For Sedimentary Geology, pp. 231–256.
Kroonenberg, S.B., Abdurakhmanov, G.M., Badyukova, E.N., van der Borg, K., Kalashnikov, A., Kasimov, N.S., Rychagov, G.I., Svitoch, A.A., Vonhof, H.B., Wesselingh, F.P., 2007. Solar-forced 2600 BP and Little Ice Age highstands of the Caspian Sea. Quaternary International 173–174, 137–143.
Lahijani, H., Tavakoli, V., 2012. Identifying provenance of South Caspian coastal sediments using mineral distribution pattern. Quaternary International 261, 128–137.
Lahijani, H.A.K., Tavakoli, V., Amini, A.H., 2008. South Caspian River Mouth configuration under human impact and sea level fluctuations. Environmental Sciences 5 (2), 65–86.
Leroy, S.A.G., 2010. Palaeoenvironmental and palaeoclimatic changes in the Caspian Sea region since the Lateglacial from palynological analyses of marine sediment cores. Geography, Environment, Sustainability 2, 32–41.
Leroy, S.A.G., Marret, F., Giralt, S., Bulatov, S.A., 2006. Natural and anthropogenic rapid changes in the Kara-Bogaz Gol over the last two centuries by palynological analyses. Quaternary International 150, 52–70.
Leroy, S.A.G., Marret, F., Gibert, E., Chalié, F., Reyss, J.-L., Arpe, K., 2007. River inflow and salinity changes in the Caspian Sea during the last 5500 years. Quaternary Science Reviews 26, 3359–3383.
Leroy, S.A.G., Lahijani, H.A.K., Djamali, M., Naqinezhad, A., Moghadam, M.V., Arpe, K., Shah-Hosseini, M., Hosseindoust, M., Miller, Ch.S., Tavakoli, V., Habibi, P., Naderi Beni, M., 2011. Late Little Ice Age palaeoenvironmental records from the Anzali and Amirkola lagoons (south Caspian Sea): vegetation and sea level changes. Palaeogeography, Palaeoclimatology, Palaeoecology 302, 415–434.
Leroy, S.A.G., Kakroodi, A.A., Kroonenberg, S.B., Lahijani, H.A.K., Alimohammadian, H., Nigarov, A., 4 March. 2013. Holocene vegetation history and sea level changes in the SE corner of the Caspian Sea: relevance to SW Asia climate. Quaternary Science Reviews.
Lewis, J., Hallett, R., 1997. *Lingulodinium polyedrum* (*Gonyaulax polyedra*) a blooming dinoflagellate. In: Ansell, A.D., Gibson, R.N., Barnes, M. (Eds.), Oceanography and Marine Biology: an Annual Review, vol. 35. UCL Press, London, pp. 97–161.
Loeblich, A.R., Tappan, H., 1987. Foraminiferal Genera and Their Classification. Van Nostrand Reinhold, New York, p. 1182.
Londeix, L., Herreyre, Y., Turon, J.-L., Fletcher, W., 2009. Last Glacial to Holocene hydrology of the Marmara Sea inferred from a dinoflagellate cyst record. Review of Palaeobotany and Palynology 158, 52–71.
Makhlough, A., Nasrollahzadeh, H.S., Pourgholam, R., Rahmati, R., 2011. The introduction of toxic and harmful new species of phytoplankton in the Iranian costal water of the southern Caspian Sea. Journal of Biology Science Lahijan 5 (2), 77–93 (in Persian).
Marret, F., Zonneveld, K.A.F., 2003. Atlas of modern organic-walled dinoflagellate cyst distribution. Review of Palaeobotany and Palynology 125, 1–200.
Marret, F., Leroy, S., Chalié, F., Gasse, F., 2004. New organic-walled dinoflagellate cysts from recent sediments of central Asian seas. Review of Palaeobotany and Palynology 129, 1–20.
Marret, F., Mudie, P., Aksu, A., Hiscott, R.N., 2009. A Holocene dinocyst record of a two-step transformation of the Neoeuxinian brackish water lake into the Black Sea. Quaternary International 197, 72–86.
McCarthy, F.M.G., Mudie, P.J., 1998. Oceanic pollen transport and pollen:dinocyst ratios as markers of late Cenozoic sea level change and sediment transport. Palaeogeography, Palaeoclimatology, Palaeoecology 138, 187–206.
Mertens, K., et al., 2009. Process length variation in cysts of a dinoflagellate, *Lingulodinium machaerophorum*, in surface sediments: investigating its potential as salinity proxy. Marine Micropaleontology 70, 54–69.
Mertens, K.N., Bradley, L.R., Takano, Y., Mudie, P.J., Marret, F., Aksu, A.E., Hiscott, R.N., Verleye, T.J., Mousing, E.A., Smyrnova, L.L., Bagheri, S., Mansor, M., Pospelova, V., Matsuoka, K., 2012. Quantitative estimation of Holocene surface salinity variation in the Black Sea using dinoflagellate cyst process length. Quaternary Science Reviews 39, 45–59.
Mudie, P.J., Leroy, S.A.G., Marret, F., Gerasimenko, N., Kholeif, S.E.A., Sapelko, T., Filipova-Marinova, M., 2011. Non-pollen palynomorphs: indicators of salinity and environmental change in the Caspian-Black Sea-Mediterranean Corridor. In: Buynevich, I., Yanko-Hombach, V., Gilbert, A.S., Martin, R.E. (Eds.), Geology and Geoarchaeology of the Black Sea Region: Beyond the Flood Hypothesis, Geological Society of America Special Paper 473, pp. 89–115.
Naderi Beni, A., Lahijani, H., Mousavi Harami, R., Arpe, K., Leroy, S.A.G., Marriner, N., Berberian, M., Ponel, V.A., Djamali, M., Mahboubi, A., Reimer, P., 2013a. Caspian sea level changes during the last millennium: historical and geological evidences from the south Caspian Sea. Climate of the Past.
Naderi Beni, A., Lahijani, H., Moussavi Harami, R., Leroy, S.A.G., Shah-Hosseini, M., Kabiri, K., Tavakoli, V., 2013b. Development of spit-lagoon complexes in response to Little Ice Age rapid sea-level changes in the central Guilan coast, South Caspian Sea, Iran. Geomorphology 187, 11–26.
Nadirov, R.S., Bagirov, E., Tagiyev, M., Lerche, I., 1997. Flexural plate subsidence, sedimentation rates, and structural development of the super-deep South Caspian Basin. Marine and Petroleum Geology 14, 383–400.
NASA, no date. http://data.giss.nasa.gov/gistemp/ (last accessed 09.03.13.).
Nasrollahzadeh, H.S., Din, Z.B., Foong, S.Y., Makhlough, A., 2008a. Trophic status of the Iranian Caspian Sea based on water quality parameters and phytoplankton diversity. Continental Shelf Research 28, 1153–1165.
Nasrollahzadeh, H.S., Din, Z.B., Foong, S.Y., Makhlough, A., 2008b. Spatial and temporal distribution of macronutrients and phytoplankton before and after the invasion of the ctenophore, *Mnemiopsis leidyi*, in the Southern Caspian Sea. Chemistry and Ecology 24 (4), 233–246.
Nasrollahzadeh, H.S., Maklough, A., Pourgholam, R., Vahedi, F., Qanqermeh, A., Foong, S.Y., 2011. The study of *Nodularia spumigena* bloom event in the southern Caspian Sea. Applied Ecology and Environmental Research 9 (2), 141–155.
Nezlin, N.P., 2005. Patterns of seasonal and interannual variability of remotely sensed chlorophyll. Environmental Chemistry 5P, 143–147.
Omrani Rekavandi, H., Sauer, E.W., Wilkinson, T., Safari Tamak, E., Ainslie, R., Mahmoudi, M., Griffiths, S., Ershadi, M., Jansen Van Rensburg, J., Fattah, M., Ratcliffe, J., Nokandeh, J., Nazifi, A., Thomas, R., Gale, R., Hoffmann, B., 2007. An imperial frontier of the Sasanian Empire: further fieldwork at the Great Wall of Gorgan. Iran 45, 95–136.
Patimar, R., 2008. Fish species diversity in the lakes of Alma-Gol, Adji-Gol, and Ala-Gol, Golestan province, Northern Iran. Journal of Ichthyology 48 (10), 911–917.
Patimar, R., Yousefi, M., Hosieni, S.M., 2009. Age, growth and reproduction of the sand smelt Atherina boyeri Risso, 1810 in the Gomishan wetland – southeast Caspian Sea. Estuarine, Coastal and Shelf Science 81, 457–462.
Pierret, M.C., Chabaux, F., Leroy, S.A.G., Causse, C., 2012. A record of Late Quaternary continental weathering in the sediment of the Caspian Sea: evidence from U-Th, Sr isotopes, trace element and palynological data. Quaternary Science Reviews 51, 40–55.
Reyss, J.-L., Schmidt, S., Legeleux, F., Bonte, P., 1995. Large, low background well-type detectors for measurements of environmental radioactivity. Nuclear Instruments and Methods A 357, 391–397.
Schumacher, B.A., 2002. Methods for the Determination of Total Organic Carbon (TOC) in Soils and Sediments. US Environmental Protection Agency, Las Vegas, NV.
Sgarrella, F., Moncharmont Zei, M., 1993. Benthic foraminifera of the Gulf of Naples (Italy): systematic and autoecology. Bollettino della Societa Paleontologica Italiana 32, 145–264.
Soloviev, D., 2005. . Identification of the Extent and Causes of Cyanobacterial Bloom in September–October 2005 and Development of the Capacity for Observation and Prediction of HAB in the Southern Caspian Sea Using Remote Sensing Technique. http://caspian.iwlearn.org/caspian-1/anomalous-algal-bloom/anomalous-algal-bloom. http://www.caspianenvironment.org/newsite/DocCenter/2006/HABrepFinalFull_corrected_compressed_pictures.doc (last accessed 23.06.12.).
Sorrel, P., Popescu, S.-M., Head, M.J., Suc, J.P., Klotz, S., Oberhänsli, H., 2006. Hydrographic development of the Aral Sea during the last 2000 years based on a quantitative analysis of dinoflagellate cysts. Palaeogeography, Palaeoclimatology, Palaeoecology 234 (2–4), 304–327.
Tagiyev, M.F., Nadirov, R.S., Bagirov, E.B., Lerche, I., 1997. Geohistory, thermal history and hydrocarbon generation history of the north-west South Caspian basin. Marine and Petroleum Geology 14, 363–382.
Tudryn, A., Chalié, F., Lavrushin Yu, A., Antipov, M.P., Spiridonova, E.A., Lavrushin, V., Tucholka, P., Leroy, S.A.G., 2012. Late Quaternary Caspian Sea environment: Late Khazarian and Early Khvalynian transgressions from the lower reaches of the Volga river. Quaternary International 292, 193–204.
Tuzhilkin, V.S., Kozarev, A.N., 2005. Thermohaline structure and general circulation of the Caspian Sea waters. In: Kostianoy, A., Kosarev, A. (Eds.), The Caspian Sea Environment. Springer, Berlin Heidelberg, pp. 33–57.
USDA, no date. http://www.pecad.fas.usda.gov/cropexplorer/global_reservoir/gr_regional_chart.aspx?regionid=stans&reservoir_name=Caspian (last accessed 09.03.13.).
Verleye, T., Mertens, K.N., Louwye, S., Arz, H.W., 2009. Holocene Salinity changes in the southwestern Black Sea: a reconstruction based on dinoflagellate cysts. Palynology 33, 77–100.
Voronina, E., Polyak, L., de Vernal, A., Peyron, O., 2001. Holocene variations of sea-surface conditions in the southeastern Barents Sea, reconstructed from dinoflagellate cyst assemblages. Journal of Quaternary Science 16 (7), 717–726.
Zaker, N.H., Ghaffari, P., Jamshidi, S., 2007. Physical study of the southern coastal waters of the Caspian Sea, off Babolsar, Mazandaran in Iran. Journal of Coastal Research 50, 564–569.
Zaker, N.H., Ghaffari, P., Jamshidi, S., Nouranian, M., 2011. Currents on the Southern Continental Shelf of the Caspian Sea off Babolsar, Mazandaran, Iran. Journal of Coastal Research 64, 1989–1997.
Zenkevitch, L.A., 1963. Biology of the Seas of the USSR. George Allen and Unwin Ltd, London.
Zonneveld, K.A.F., Marret, F., Versteegh, G.J.M., Bogus, K., Bonnet, S., Bouimetarhan, I., Crouch, E., de Vernal, A., Elshanawany, R., Edwards, L., Esper, O., Forke, S., Grøsfjeld, K., Henry, M., Holzwarth, U., Kielt, J.F., Kim, S.Y., Ladouceur, S., Ledu, D., Chen, L., Limoges, A., Londeix, L., Lu, S.H., Mahmoud, M.S., Marino, G., Matsouka, K., Matthiessen, J., Mildenhal, D.C., Mudie, P., Neil, H.L., Pospelova, V., Qi, Y., Radi, T., Richerol, T., Rochon, A., Sangiorgi, F., Solignac, S., Turon, J.L., Verleye, T., Wang, Y., Wang, Z., Young, M., 2013. Atlas of modern dinoflagellate cyst distribution based on 2405 data points. Review of Palaeobotany and Palynology 191, 1–197.